A Database For The Etching of LGS in H_2SO_4:H_2O

C.R. Tellier, M. Akil, T.G. Leblois
Institute FEMTO-ST
Department Chronométrie Electronique Piézoélectricité
Besançon, France
ctellier@ens2m.fr

Abstract— **twelve differently oriented LGS plates were etched in a H_2SO_4: H_2O solution. 2D etching shapes (profilometry traces and out-of-roundness profiles) were analyzed to determine the dissolution constants that characterize the anisotropy. After adjustments theoretical etching shapes derived from the self-elaborated simulator TENSOSIM were found to be in close agreement with experimental shapes supporting the validity of the present database.**

I. INTRODUCTION

The LGS crystal that offers high coupling coefficients [1,2] can be considered as an alternative material to quartz crystal for BAW resonators. However Quartz is also a crystal for MEMS and in the last decade several works [3-5] were devoted to quartz resonating structures fabricated by wet micromachining. A previous study [6] on wet etching of LGS in H_2SO_4:H_2O etchant has given evidence for a chemical attack governed by orientation. However to our knowledge up to now there is a lack of database capable to characterize the anisotropic etching of LGS. To reply to this lack this paper focuses on the determination of the dissolution constants describing the anisotropy of etching shapes. The first part is devoted to the experimental results related to twelve differently oriented LGS plates and emphasis is placed on (1) out-of-roundness profiles that illustrate modifications of the starting circular contour of LGS plates, (2) surface profilometry traces. A systematic analysis of the 2D etching shapes is performed in the second part that leads to the determination of a database (dissolution constants). The third part deals with numerical simulations of etching shapes using the simulator TENSOSIM that works with the proposed database.

II. EXPERIMENTALS

A. Experimental Details

Twelve thin circular plates (1500 µm thick) were cut from a LGS ingot. All plates are singly rotated plates. The angle of rotation θ about the X axis takes positive and negative values in order to describe the whole space. Values retained for θ are 0°, ± 15°, ± 25°, ± 35°, ± 45°, ± 55°, ± 65° and 90°. In the following a cut with $\theta = \pm \theta_o$ is named $Y \pm \theta_o$.

Let us also recall that with this convention the Y and Z cuts correspond respectively to θ =0° and θ =90° respectively. The circular contour and one of the two faces of LGS plates were lapped and then mechanically polished. Moreover in order to observe rapidly the formation of dissolution figures on etched surfaces the other face of plates is only lapped. The etchant is a H_2SO_4:H_2O solution with composition 20:1. Plates were etched at a constant temperature of 353 K (accuracy of about ± 1 K). Experimental details on surface topography measurements are given elsewhere [6]. The changes in shape of the starting circular section of plates were studied using a Talyrond® analyzer that generates the out-of-roundness profile at a magnified scale with the superimposed least mean square circle.

B. Surface Profilometry Traces

It was shown [6] for LGS plates the etching generates dissolution figures whose shape depends on the cut and that the geometrical features of a profilometry trace made on an etched plate are determined by the direction of the trace. Consequently we have chosen two specific directions of alignment for the profilometry traces (1) The X direction that is common at all cuts investigated here, (2) The direction that lies perpendicular to the X axis that is to say the rotated Z' axis. As example, Fig. 1 gives some X and Z' profilometry traces. As observed for dissolution process governed by orientation the various profilometry traces exhibit different shapes. Convex (Fig. 1C) or concave (Fig. 1D) background may be formed depending on the cut and on the trace direction. But more complex geometrical features can be depicted on Figs 1c and 1C where two consecutive curved convex and concave (or concave-convex) elements constitute the characteristic shape of traces. Surface profiles can be also composed of quasi linear elements (Figs. 1b and 1B). Several works have given evidence [7-9] that: (1) only elements with diverging trajectories contribute to the final surface profile, (2) the nature concave or convex of curved elements that compose a surface profile is intimately connected to the number and the nature (maximum or minimum) of extrema of the dissolution slowness lying in the vicinity of the reference dissolution slowness of the cut L_o. Consequently an easy prediction of

DGA, Paris

surface profile shapes remains impossible in absence of complete database.

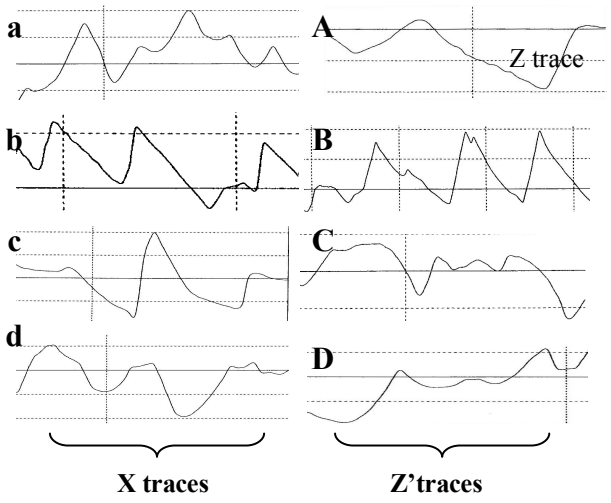

Figure 1. Some X and Z' profilometry traces made on various plates. Traces (a,A), (b,B), (c,C) and (d,D) are for Y+15, Y+35, Y-35 and Y-55 cuts respectively.

C. *Out of Roundness Profiles*

Out-of-roundness profiles (ORP) corresponding to various $Y\pm\theta_o$ cross-sectional planes are displayed in Fig. 2. Note that: (1) ORP associated with Y–25, Y–45, Y–65 and Z cuts are rotated by 180° with respect to other ORP, (2) the crystallographic X direction lies vertically on the graphs.

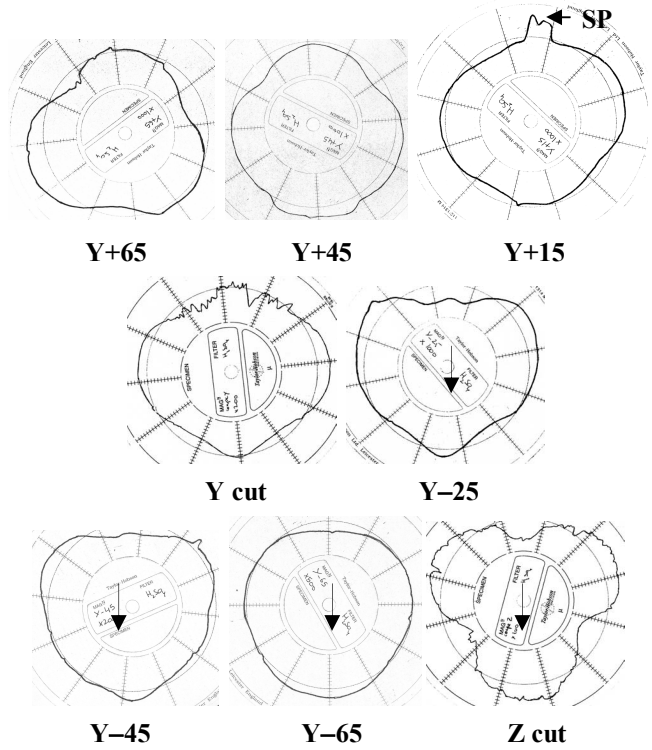

Figure 2. Out-of-roundness profiles related to various cuts.

The different ORP show a "mirror" symmetry with respect to the X axis. Moreover ORP are composed of successive peaks and valleys that are formed when the dissolution slowness passes through maximums and minimums respectively. Hence an ORP is correlated to the polar plot of the dissolution slowness in the corresponding cross sectional plane $Y\pm\theta_o$.

III. THE DATABASE

A. *The Theoretical Framework*

Let us recall that in the KT model we associate at a surface element of orientation (φ,θ) (i.e. φ and θ are the angles of cut) a dissolution slowness vector **L** that characterizes the anisotropy of the dissolution process. The vector **L** is related to parameters that can be determined experimentally in such a way [5] that its magnitude $L(\varphi,\theta)$ is equal to the reciprocal of the etch rate $R(\varphi,\theta)$ and that its direction coincides with that of the unit inward normal **n** to the surface element. So when the orientation of the surface element varies the extremity of the vector **L** describes in space a representative surface called the dissolution slowness surface. The KT model constitutes a tensorial model because to express the analytical equation $L(\varphi,\theta)$ of the dissolution slowness

$$L(\varphi,\theta) = L(n_1,n_2,n_3) = D_o + D_i n_i + D_{ij} n_i n_j + D_{ijk} n_i n_j n_k + \ldots \quad (1)$$

we introduce dissolution constants D_o, D_i, D_{ij}, D_{ijk},… that can be identified as the independent constants of dissolution tensors of rank $N_R = 0, 1, 2, 3,\ldots$ etc.

In Eq. (1) n_1, n_2 and n_3 are the Cartesian components of the inward normal **n**. The number of dissolution constants is reduced by cyclic permutation of subscripts and by the crystal symmetry [5]. Hence in this framework the dissolution slowness surface contains the symmetry of the point group. This model applies if the dissolution is governed by orientation only and in this case the trajectory of a surface element within the crystal during the dissolution follows a straight line so that we can associate a displacement vector **P** to the surface element. The major advantage of this model is that it is possible [10] to determine the Cartesian components of **P** from the Eq. (1). Consequently the KT model is adapted to a numerical construction of etching shapes [7-9]. The self-elaborated simulator TENSOSIM that is based on the framework of the KT model uses the dissolution constants as database.

B. *Determination of the Database*

The dissolution constants are extracted from experimental results on: (1) changes in the dissolution slowness, (2) experimental 2D etching shapes. But we have to overcome some difficulties because we cannot evaluate the true dissolution slowness corresponding to a perfectly flat crystallographic plane since etched surfaces are covered by dissolution figures. So the major part of the procedure is based on an analysis of etching shapes that involves two main steps. In the first step of this procedure we investigate experimental 2D etching shapes such as out-of-roundness profiles and 2D profilometry traces because: (1) an ORP related to a given cross-section (angles of cut φ_o and θ_o)

constitutes a crude image of the polar diagram of the dissolution slowness lying in the same section, (2) surface profiles give complementary information on a small angular sector of the dissolution slowness even if the analysis gives better conclusions when elongated dissolution figures develop on etched surfaces. To overcome these difficulties an iterative procedure described elsewhere [7] is adopted. In this procedure we compare at each step the experimental 2D etching shapes to simulations. The procedure is stopped when a good agreement is observed so that the proposed database is supposed to be correctly adjusted. The selected database is composed essentially of dissolution constants associated with tensors whose rank N_R is in the range 7 to 10. Effectively previous works [3,9] showed that tensors of relatively high ranks ($N_R \geq 8$) are needed to produce the anisotropy observed for crystals such as quartz and silicon. The selected database gives the polar graphs of the dissolution slowness displayed in Fig. 3. On these polar graphs the X axis is vertical so considering the polar graph related to the Y cut we can observe that: (1) the two faces of an X plane dissolve with different etch rates, (2) the Z cut corresponds to the cut with the larger dissolution slowness. These observations agree with previous results [6].

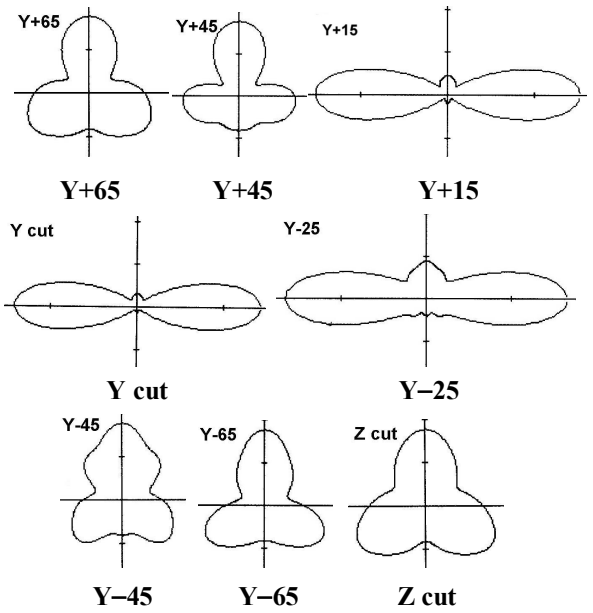

Figure 3. Some plots of the dissolution slownes lying in Y ± θ_o cross sections.

IV. SIMULATIONS

A. Simulations of ORP

When we perform simulation of etched ORP we assume that the starting cross-section of a cylindrical crystal is composed of successive linear segments formed by intersecting planes that are tangent to the starting circular section. Consequently the knowledge of the entire polar graph of **L** lying in the cross-sectional plane enables us to derive simulations of etched cross-section and of ORP. It follows that we are now concerned with an angular sector of 360°. At this point it should be important to remark that the contour of the starting circular shape is convex. Hence in terms of dissolution criteria [5,7] the etching shape of a starting 2D convex profile must be primarily determined by minimums in the corresponding polar diagram of **L**. Consequently the etched cross-section involves only profile elements whose dissolution slowness remains in the close vicinity of minimums L_{mi} in the cross-sectional polar graph of **L**. It is clear that peaky minimums inducing markedly diverging trajectories of profile elements must yield crudely linear portions. As a result the ORP exhibits a deep valley. In contrast smooth minimums produce the curved portions of the etched contour and the less accentuated valleys in ORP.

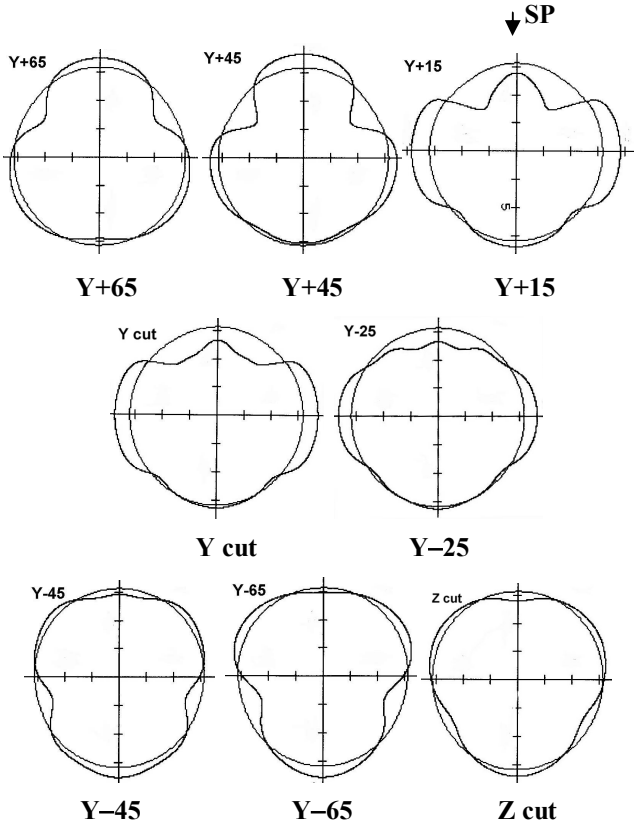

Figure 4. Theoretical Out-of-roundness profiles related to the various cuts shown in Fig. 2.

Figure 4 shows simulated ORP related to various cuts. Note that the theoretical graphs are presented to ensure a direct comparison with experimental graphs of Fig. 3. Examination of these figures reveals several features:

- As expected a theoretical ORP shows progressive changes in etching shape when the angle of cut θ_o varies from –90° to 90°.
- A satisfactory agreement between simulated etching shapes of ORP and experimental shapes. The best agreements are obtained for Y+65, Y, Y–25, Y–45, and Z cuts. Moreover the relatively sharp peak (SP) that can be depicted on the Y+15 ORP of Fig. 2 seems effectively correspond to the SP peak of the theoretical Y+15 ORP (Fig. 4).

- Comparison of theoretical ORP with the polar diagrams of Fig. 3 shows that in fact an ORP profile resemble to corresponding polar graph of **L**. Hence ORP allow us to evaluate with a sufficient accuracy orientation (φ_{mi}, θ_{mi}) of planes associated with minimums m_i in the polar graph. However the relative amplitude of successive maximums and minimums in the dissolution slowness cannot be evaluated precisely using experimental ORP.

Owing to the observed agreement it is justified to extend the simulation procedure to surface profiles.

B. Framework for Simulations of Surface Profiles

In contrast with ORP simulations the simulation for a profilometry trace works with a small angular sector on the corresponding polar plot of **L**. The only difficulty is to recognize the polar plot used in simulation because this polar plot depends on the direction of trace. For simplicity consider a starting triangular profile with initial slopes of ± 20°. A trace aligned along the X axis (Fig. 5a) lies in the plane perpendicular to the reference plane X, Z' (angle of cut θ_o and dissolution slowness $\mathbf{L_o}$) that is to say in the cross-sectional plane X, Z* with angle of cut θ_o+90°. To simulate the final etching shape of the X trace we have to: (1) use the X, Z* polar graph, (2) work with an angular sector of 40° centered on the reference dissolution slowness $\mathbf{L_o}$ that lies parallel to the Z* axis. If we turn attention to the polar graphs of Fig. 3 where the X axis is vertical it is clear that the reference dissolution slowness is horizontal. Moreover the face is irrelevant because of the two-fold symmetry about the X axis. Figure 6 indicates clearly how locate $\mathbf{L_o}$ on the corresponding polar plot.

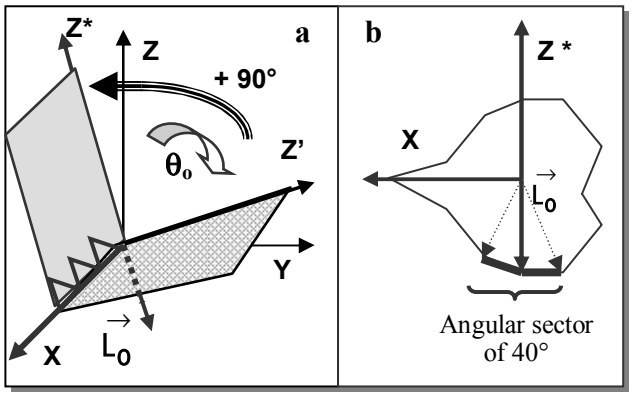

Figure 5. The case of an X trace : (a) determination of the cross-sectional plane X, Z* and (b) location of the reference dissolution slowness.

Let us now turn attention to Z' surface profilometry traces. Figure 7a indicates that all Y ± θ_o reference planes have the same cross-sectional plane. This cross-sectional plane is identified to be the X cut (Y,Z plane). As the angle of cut θ varies the reference dissolution slowness $\mathbf{L_o}$ that rotates about the X axis moves on the cross sectional polar graph (Fig. 7b). As a result the etching shape of Z' traces must changes progressively with θ.

TABLE I. CORRESPONDENCE BETWEEN REFERENCE PLANE AND CROSS-SECTIONAL PLANE

Correspondence X, Z cut ↔ X, Z* cut	
Y+65	Y–25
Y+45	Y–45
Y+15	Y–75*
Y cut	Z cut

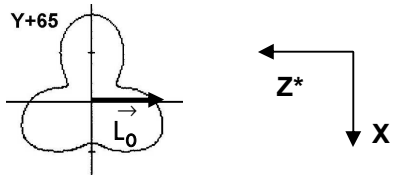

Figure 6. Location of the reference dissolution slowness (related to the Y–25 cut) on the cross-sectional plane Y+65.

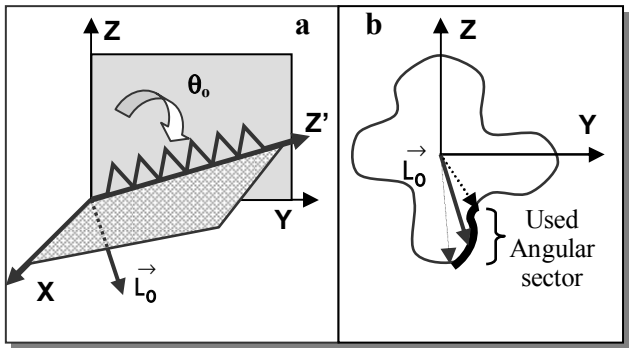

Figure 7. The case of a Z' trace : (a) determination of the cross-sectional plane X, Z* and (b) location of the reference dissolution slowness.

C. Simulations of Z' Traces

To simulate the etching of lapped surfaces we use the starting surface profile of Fig. 8 that is composed of successive linear elements with slopes in the range – 20°, +20°. With these slope it is reasonable to assume that this surface profile represent a trace made on a rough surface.

Figure 8. The starting surface profile

Figure 9 gives experimental and simulated Z' traces as derived by the simulator using the same etching duration Δt (Δt = 20 arbitrary units) for all surface profiles. Figure 9 calls for two remarks:

- Firstly, the etching shape of Z' traces varies progressively when the angle of cut θ decreases from 90° (Z cut) to – 65°(Y–65 cut). In particular we observe that a Z' trace passes successively through a

concave background (θ = 90°), a convex background for θ in the vicinity of + 45°, a somewhat concave profile for the Y cut (θ = 0°), a relatively flat convex profile for θ = – 45° to clearly return to a concave background for the Z cut (θ = –90°). Moreover it appears that the simulation predicts the formation of alternate convex-concave surface profiles for orientations between those leading to the development of concave and convex backgrounds (see Figs. 9d and 9f for example).

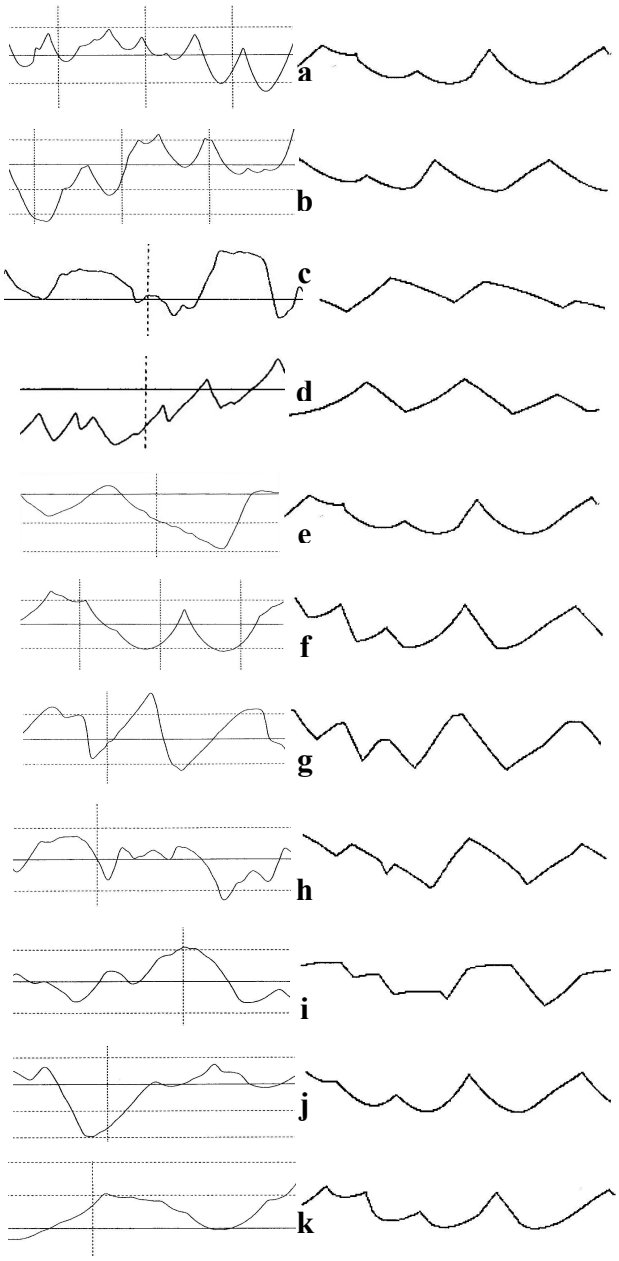

Figure 9. Experimental and theoretical Z' traces made on: (a) Z, (b) Y+65, (c) Y+45, (d) Y+35, (e) Y+15, (f) Y, (g) Y-15, (h) Y-35, (i) Y-45, (j) Y-55 and (k) Y- 65 plates.

- Secondly, there is a satisfactory resemblance between experimental and theoretical Z' traces. The agreement seems to be less good for the Y–45 plate for which the simulation generates a convex Z' profile with flat plateaus. At this point it is important to outline that the shape of a simulated trace may for some orientations be strongly dependent on the etching time duration Δt. Figure 10 gives evidence for a time dependent behavior in the case of the Y–45 plate.

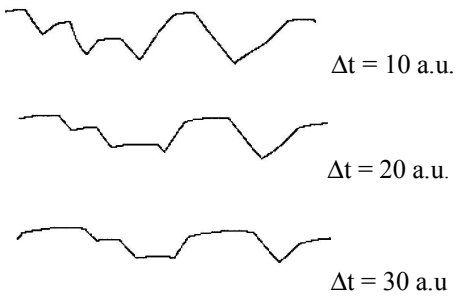

Figure 10. Evolution with etching time Δt of a Z' trace made on Y-45 plate.

As noticed in section IV.*B* it is possible to connect the etching shape of Z' traces to the polar plot of **L** related to the X cut. To verify this connection a zoomed view of the X polar plot is drawn in Fig.11. In addition values θ_M and θ_m of the angle of cut θ for which the dissolution slowness passes through maximums (M) and minimums (m) are listed in Table II. Turning attention to Figs. 9 and 11 and to table II it appears that concave and convex backgrounds develop when the reference dissolution slowness corresponds to a maximum and to a minimum respectively. The formation of a Z' profile with alternate concave-convex shape is caused by the presence of a maximum and a minimum in the working angular sector of 40° or in proximity of this sector. The somewhat theoretical convex-convex that develops on the Y-35 plate is due to the presence of three extremums (two minimums at –41° and –14° and maximum at –38°). All these features are in accord with dissolution criteria [5,7].

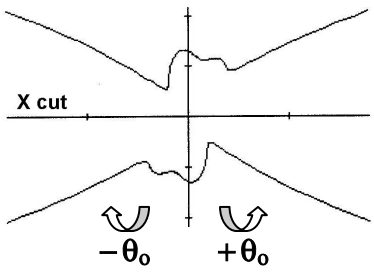

Figure 11. Zoomed representation of the polar polar of **L** related to the X cut

TABLE II. ANGULAR POSITION S OF EXTREMA IN THE X POLAR PLOT

Maximums, angle θ_M (°)	Minimums, angle θ_m (°)
– 90°, –31°, 3°, 90°	– 41°, – 14°, 38°

D. *Simulations of X Traces*

Experimental and theoretical shapes of the various X traces are shown on Fig. 12. This figure calls for two observations:

- The theoretical traces are in close accord with experimental X traces. In fact the accord covers all the $Y \pm \theta_o$ cuts investigated in this study.
- In contrast with Z' traces experimental and theoretical shapes of X traces do not show a continuous evolution with the angle of cut θ. In practice we observe that profiles exhibit mostly concave shapes. An X profile with alternate shape is without ambiguity formed on the Y+45 plate.

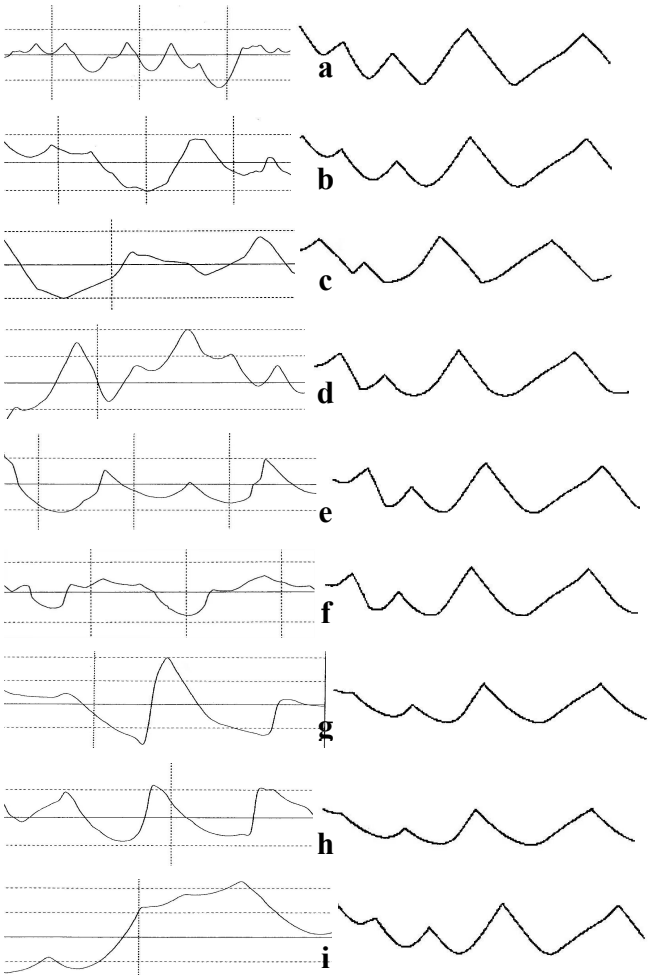

Figure 12. Experimental and theoretical X traces made on: (a) Z, (b) Y+65, (c) Y+45, (d) Y+15, (e) Y, (f) Y- 15, (g) Y-35, (h) Y- 45 and (i) Y- 65 plates.

The second observation merits some comments. Effectively taking into account: (1) correspondences indicated in Table I, (2) shapes of polar plots in the vicinity of the horizontal axis (Fig. 3) it is possible to draw conclusions on theoretical shapes of X traces. These conclusions are summarized in Table III.

TABLE III. CONCLUSIONS ON X PROFILE SHAPES

Cut	shape	remarks
Y+65	Concave	Maximum active
Y+45	Concave-convex	concave and convex curvatures active
Y cut	Majority concave	Curvature near maximum more active
Y–45	Nearly concave	Maximum active
Z cut	Majority concave	concave curvature more active

V. CONCLUSION

The chemical etching of LGS in a H_2SO_4:H_2O solution is anisotropic. Hence etching shapes of ORP depend on the cut whereas shapes of surface profilometry traces are characteristic of the cut but also of the direction of traces. The database extracted from a systematic analysis of these 2D etching shapes shows that contrary to quartz the Z cut dissolves the most slowly. Using the proposed database to derive theoretical ORP from the simulator TENSOSIM gives theoretical shapes in close accord with experimental shapes. A satisfactory agreement between experiments and simulations is also obtained for 2D surface profiles. The small deviations observed for some traces may be understood in terms of development of dissolution figures with short extend in all directions. It is clear that for a further adjustment of the database it is now necessary to continue with the micromachining of 3D LGS structures.

REFERENCES

[1] M. Pereira da Cunha, D.C. Malocha, "BAW Temperature Sensitivity and coupling in langasite", IEEE Trans. UFCC, vol 49, pp 656-663, May 2002

[2] J. Bohm, R.B. Heimann, M. Hengst, R. Roewer and J. Schindler, "Czochralski growth and characterization of piezoelectric single crystals with langasite structure. Part I", J. Cryst. Growth, vol 204, pp 128-136, 1999

[3] C.R. Tellier and T.G. Leblois, "Micromachining of quartz plates: Determination of a database by combined stereographic analysis and 3D simulation of etching shapes", IEEE Trans. UFFC, Vol 47, pp 1204-1216, 2000

[4] C.R. Tellier, T. Messaoudi, T.G. Leblois and S. Durand, "Convex and concave undercuttings in the micromachining of quartz and silicon structures", Proceedings of 11th European Frequency and Time Forum, Neuchatel, Switzerland, 4-7 March 1997, pp 386-390

[5] C.R. Tellier, "Micro-usinage Chimique du Quartz : Modélisation et Contrôle par Microscopie Electronique à Balayage", *Research contract DRET 85.34.099.470.75.01*, February 1988, 169 pp

[6] M. Akil, C.R. Tellier and T.G. Leblois, "Chemical etching of LGS: Evidence for anisotropy", Proceedings of the 16th European Frequency and Time Forum, Braunschweig, Germany, 2002, CD-ROM

[7] C. Hodebourg and C.R. Tellier, "Some investigations on the anisotropy of the chemica etching of (hk0) and (hhl) silicon plates in a NaOH 35% solution. Part I: 2D etching shapes", Acive and Passive Electrocomp., vol 34, pp 31-56, 2001

[8] C.R. Tellier, T. Leblois and P.C. Maitre, "Dissolution shapes of Y-rotated quartz plates and Y sections derived from the polar diagram of the dissolution slowness", J. Mater. Sci., vol 24, pp 3029-3039, 1989

[9] C.R. Tellier, "Anisotropic etching of silicon crystals in KOH solution. Part III. Experimental and theoretical shapes for 3D structures micromachined in (hk0) plates", J. Mater. Sci. , Vol 33, pp 117-131, 1998

[10] C.R. Tellier "A three dimensional kinematic model for the dissolution of crystals", J. Cryst. Growth , vol 96, pp 450-452, 1989